Factors promoting hot-exciton formation during charge recombination in organic thin films

Thomas Pope [*] and Thomas Penfold [†]

Chemistry, School of Natural and Environmental Sciences, Newcastle University, Newcastle upon Tyne NE1 7RU, United Kingdom

The outcome of excited-state processes is strongly dependent on initial conditions, i.e., the nature of the state arising from excitation. The physics of photoexcitation and the nature of the excited states generated are well established and applied routinely in the exploration of photochemical mechanisms and the interpretation of laser experiments across a broad range of molecules and materials. However, despite its importance in emerging technologies such as organic light-emitting diodes (OLEDs), the nature of excited states formed by electrical excitation is much less understood. In this paper, we use kinetic Monte Carlo (KMC) simulations to reveal that during charge recombination there is a substantial probability of forming higher-lying excited states with >0.5 eV excess energy compared to the lowest excited state. The probability of these hot-exciton pathways depends on the energy gap between the states and the intrinsic energetic disorder in the system. Our simulations also reveal the concept of *electrical selection*, in that only higher-lying excited states exhibiting HOMO $\rightarrow$ x or x $\rightarrow$ LUMO character (where "HOMO" refers to the highest occupied molecular orbital and "LUMO" refers to the lowest unoccupied molecular orbital) can be formed. Importantly, the potential to form these higher-lying excited states is likely to have significant implications for the lifetime of OLEDs, especially those operating in the blue, as the excess energy will push the core components closer to the damage thresholds, increasing the probability of degradation.

I. INTRODUCTION

Upon interaction with light, a molecule can be transferred into an electronically excited state, the precursor to many core chemical events such as charge transfer [1], energy transfer [2], and dissociation [3,4]. Crucially, the nature of the excited state and the ensuing dynamics are strongly dependent on the characteristics of the radiation source used [5] and therefore an extensive research effort has focused on determining the role of intensity [6,7], wavelength [8,9], and duration [10] on the initial conditions associated with the photoexcited states generated. In contrast, excited states in many emerging organic electronics technologies, such as organic light-emitting diodes (OLEDs), are generated by the electrical excitation, i.e., through the recombination of charges (electrons and holes) as they traverse the material under the influence

*thomas.pope2@newcastle.ac.uk
†tom.penfold@newcastle.ac.uk

of an external bias [11]. In such cases, it is important to recognize that the excited states formed by charge recombination are profoundly different from those formed by photoexcitation. These differences are most apparent in the importance of spin statistics for charge recombination over transition dipole moments in photoexcitation, which leads to the majority of the initially generated excitons forming in the triplet states, a process usually forbidden or only weakly allowed in the case of photoexcitation [12–15]. However, despite its importance, comparatively little is known about the initial conditions of the excited states generated upon electrical excitation.

Presently, the mechanism of charge recombination during electrical excitation is understood through simplistic empirical considerations. It is usually assumed that the charges traverse the material through the lowest unoccupied molecular orbital (LUMO) and highest occupied molecular orbital (HOMO) levels for the electrons and hole, respectively, leading to the formation of either the lowest singlet (S_1) or triplet (T_1) states. Beyond this, Li *et al.* have recently proposed a hot-exciton mechanism [16]. This relies upon the assumption that exciton formation initially occurs through the formation of a charge-transfer (CT) state [15,17,18]. In such cases, by designing molecules in which the CT states are not the lowest excited states and suppressing internal

conversion to lower-lying excited states, the authors have proposed that the charge recombination could efficiently generate excited states at higher energy [19]. In the context of OLED performance, especially for thermally activated delayed fluorescence (TADF) emitters [20,21], the formation of higher-lying excited states may open new efficient pathways for converting triplet to singlet excitons [22]. This mechanism has been used to interpret some high-performing OLED devices [23]. However, these higher energetic states may also open the pathway to degradation [24,25], especially for blue OLEDs, which currently suffer short operational lifetimes, as the emission energy of blue light (3.1 eV) is close to the dissociation energy of a typical C—N bond, which is approximately 3.2 eV, illustrating that even a small amount of excess energy could significantly increase the rate of degradation and reduce the device lifetime.

Lee *et al.* have previously identified high-energy excited states as a key source of degradation of blue OLEDs [26] but in this case, the excess energy has been generated by triplet-triplet annihilation (TTA), forming energetically hot states with double the energy of the lowest triplet state (approximately 6 eV). To overcome this, the authors included extra molecules into the device to rapidly accept the excess energy before damage is induced on the dopant or host. Overall, the short operation lifetime of blue OLEDs is usually attributed to exciton-exciton or exciton-polaron annihilation processes [27–29], which generate very high energetic states. Importantly, both of these processes rely on exciton diffusion and can, therefore, be somewhat controlled by minimizing the excited-state lifetime or guest density, reducing the density of triplet states.

In this paper, we present an alternative pathway to higher-lying exciton formation. Using kinetic Monte Carlo (KMC) simulations to study the dynamics of exciton formation by charge recombination in an organic thin film, our simulations reveal the potential for hot-exciton states to form during, not after, exciton generation. The probability of forming these high-lying excited states depends on the energy gap between the states and the intrinsic energetic disorder in the system but remains significant even for higher-lying excited states with >0.5 eV excess energy compared to the lowest excited state.

II. THEORY AND METHODS

Charge transport in organic semiconductor systems occurs via thermally assisted hopping events, which we model using a KMC approach [30]. Here, the molecules are modeled as a uniform cubic lattice of grid points, each containing a set of four energy levels (HOMO − 1, HOMO, LUMO, and LUMO + 1). Holes and electrons are distributed throughout the system, with holes distributed

on the HOMO levels and electrons on the LUMO levels, each with an initial charge density ρ_0. For a given configuration, each charged particle can hop to a site within a set radius of its origin site ($\sqrt{3}L$, where L is the spacing of the cubic grid points) and, for a hopping event from level m on site $\mathbf{i}$ to level n on site $\mathbf{j}$, there is an associated change in energy for the system $\Delta E_{\mathbf{ij}}^{mn}$. Given this change in energy, a Miller-Abrahams rate is calculated,

$$k_{\mathbf{ij}}^{mn} = \omega_0 e^{-2\gamma|\mathbf{R}_{\mathbf{ij}}|} \times \begin{cases} e^{-\Delta E_{\mathbf{ij}}^{mn}/k_B T}, & \Delta E_{\mathbf{ij}}^{mn} > 0, \\ 1, & \Delta E_{\mathbf{ij}}^{mn} \leq 0, \end{cases} \quad (1)$$

where $\mathbf{R}_{\mathbf{ij}}$ is the spatial vector between sites $\mathbf{i}$ and $\mathbf{j}$, γ is the inverse charge localization, and ω_0 is the hopping-attempt frequency of the charged particle. The KMC procedure involves calculating this rate for all possible hopping events, randomly selecting one for the resulting probability distribution of events, and updating the system accordingly. This procedure is repeated until the number of iterations N_{iter} is fulfilled. In addition, each system is generated and simulated N_{sim} times and the output parameters are taken from a statistical analysis of all simulations on each system.

To simulate the effect of uncorrelated noise arising from orientation and conformational differences between the molecules, the energy $E_{\mathbf{i}}^m$ for level m of site $\mathbf{i}$ in the system is given by the unperturbed energy of the given level and a site- and level-specific energy chosen randomly from a Gaussian density of states (DOS) of width σ, where the size of σ reflects the disorder and therefore the energy width of the states. The difference in energy due to a hopping event from level m on site $\mathbf{i}$ to level n on site $\mathbf{j}$ is given by

$$\Delta E_{\mathbf{ij}}^{mn} = \left(E_{\mathbf{i}}^m - E_{\mathbf{j}}^n\right) + \Delta E_{\mathbf{ij}}^{\text{Coul}} + \Delta E_{\mathbf{ij}}^{\text{field}}, \quad (2)$$

where ΔE^{field} is the change in energy due to the external electric field and the Coulomb term, resulting from electrostatic interaction between a charged particle and all other charged particles in the system, is given by

$$\Delta E_{\mathbf{ij}}^{\text{Coul}} = \frac{1}{\epsilon_r} \left(\sum_{\substack{k \neq j \\ k=\text{occupied}}} \frac{1}{|\mathbf{R}_{\mathbf{jk}}|} - \sum_{\substack{k \neq i \\ k=\text{occupied}}} \frac{1}{|\mathbf{R}_{\mathbf{ik}}|} \right), \quad (3)$$

where ϵ_r is the relative permittivity of the medium. In all that follows, the field is set to 5×10^5 V/cm, chosen to generate a reliable forward mobility in all systems studied, while still allowing for some diffusion. Note that at this field, the relative energy difference for an up- or down-field jump is 0.05 eV, well below the width of the Gaussian DOS and the energy gap between energy levels, so that the
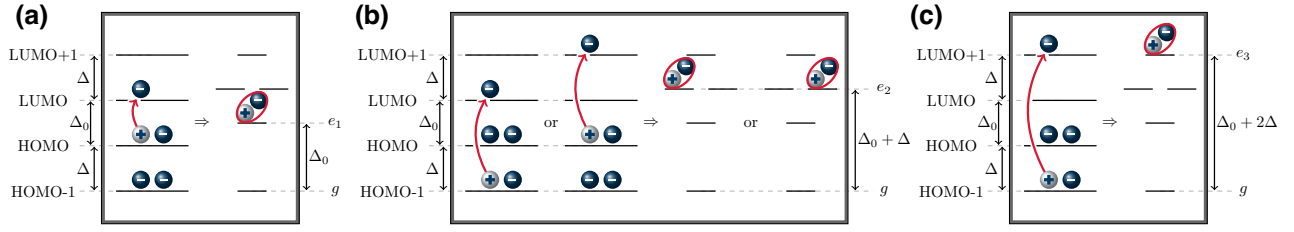
FIG. 1. A schematic of the energy levels on each site and the corresponding excitons for the (a) e_1, (b) e_2, and (c) e_3 states.

promotion of any hot excitons is due mostly to the intrinsic properties of the system and not to the applied electric field.

In addition to hopping events from site to site, a charged particle in the $HOMO - 1$ $(LUMO + 1)$ level can relax to the HOMO (LUMO) level on the same site. This rate, unless otherwise stated, is assumed to be 2 orders of magnitude higher than the hopping-attempt frequency, $k_{\mathbf{ii}}^{m0} = 100 \times \omega_0$ and so is overwhelmingly probable whenever the charge configuration allows it.

Whenever an electron and hole exist on the same site, an exciton is formed, the nature of which is governed by the energy levels of the hole and electron. Figure 1 shows the level configuration on each site and the resulting exciton configurations with their corresponding energies. The lowest-lying exciton e_1 is formed from a HOMO-to-LUMO transition. The gap, Δ_0, between these orbitals has been set to 0.4 eV throughout this work. While this would correspond to an OLED emitting at 2500 nm, this value has been chosen to encourage exciton formation and reduce the computational expense of obtaining realistic statistics from the simulations. However, despite the small energy gap, this will not change the relative population of the e_1, e_2, and e_3 states. For this, it would be the energy gaps between the $HOMO \rightarrow HOMO - 1$ and $LUMO \rightarrow LUMO + 1$ levels that would be most important, as investigated here. The first hot exciton, e_2, is formed from either a $HOMO - 1 \rightarrow LUMO$ or a $HOMO \rightarrow LUMO + 1$ transition, leading to a state with an excess energy of Δ. The

highest-lying hot exciton, e_3, is formed from a $HOMO - 1 \rightarrow LUMO+1$ transition and has an excess energy of 2Δ. Throughout this work, the spin state of the excitons is not ascribed, as the mechanism of interest is independent of spin. The model of excitonic states developed on each site represents a molecule with three close-lying excited states, all of similar character, where only the relative energetics control the populations. Any differences associated with cross sections for recombination for states of different character, such as charge transfer and locally excited states, are not considered [15].

III. RESULTS

Figure 2(a) shows the total excitons generated during the KMC simulations as a function of σ, the width of the on-site Gaussian DOS, for different separations between the excited states, Δ. Figure 2(b) shows the proportion of these excitons that populate higher-lying excited states. In Fig. 2, we only consider the e_2 hot excitons, as the e_3 states are not populated, as discussed in more detail below. As expected, the fraction of hot excitons reduces as Δ increases, which is due to the higher barrier between a HOMO (LUMO) level on one molecule and the $HOMO - 1$ $(LUMO + 1)$ level on its neighbor. Indeed, if one considers the most favorable scenario for the promotion of an e_2 state—that of a forward hop onto an occupied site—then, discounting the effect of the Gaussian DOS and the negligible change in the field, the probability of forming the e_2 state is $\propto e^{-\Delta/k_B T}$, which quickly tends to zero as Δ increases. Despite this, there remains >1% of the excitons formed populating higher-lying excited states for an energy gap of 0.5 eV and $\sigma \geq 0.15$ eV. Here, the Gaussian DOS generates a significant overlap with neighboring sites, allowing the charge particles to circumnavigate the energy barrier to e_2 formation.

Figure 2(c) translates the population of hot excitons into a density, as a function of both Δ and σ. While this illustrates a significant density of higher-lying excited states within our present simulations to assess their relevance, especially within the context of degradation, they must be contrasted with competing mechanisms. Here, we express the kinetics of four degradation mechanisms; exciton-polaron, exciton-exciton, and cold and hot exciton,

TABLE I. A list of the values of all the free parameters given in the KMC calculation.

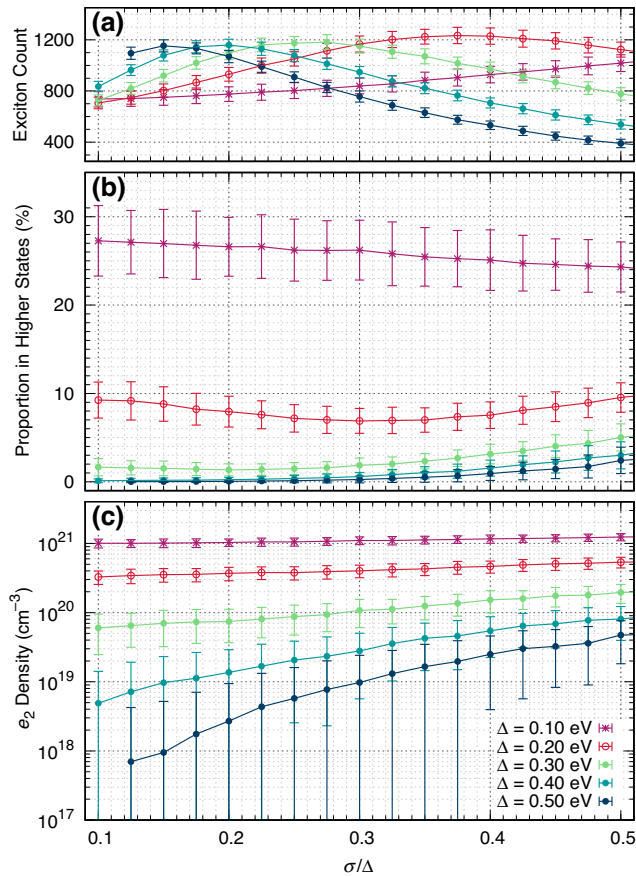| Parameter	Description	Value	Units
Δ_0	HOMO-LUMO gap	0.4	eV
ρ_0	Initial charge density	10^{-3}	nm^{-1}
γ	Inverse charge localization	2.0	nm^{-1}
L	Lattice spacing	1	nm
F	Applied field	5×10^5	V/cm
ω_0	Hopping-attempt frequency	10^{12}	s^{-1}
ϵ_R	Relative permittivity	3.0	ϵ_0
N	System dimensions	200^3	Grid points
N_{iter}	System iterations	10^5	Iterations
N_{sim}	System simulation	88	Simulations

FIG. 2. (a) The number of excitons formed as a function of the width of the Gaussian DOS for a range of Δ. (b) The population of the higher-lying excitons formed as a function of the width of the Gaussian DOS for a range of Δ. (c) The density of e_2 states formed as a function of the width of the Gaussian DOS for a range of Δ.

where $[\dot{F}]$ is the change of the fragmented or defect sites with time. The rate equations for each process, assuming that they only involve the concentration of triplet excitons ($[T]$), can be written as follows:

$$[\dot{F}]_{tt} = \Phi^d_{tt} k_{tt} [T]^2, \tag{4}$$

$$[\dot{F}]_{tp} = \Phi^d_{tp} k_{tp} [T] [p^{\pm}], \tag{5}$$

$$[\dot{F}]_{ce} = \Phi^d_{ce} k_{ce} [T_{ce}], \tag{6}$$

$$[\dot{F}]_{he} = \Phi^d_{he} k_{he} [T_{he}]. \tag{7}$$

Equation (4) describes the rate of degradation products arising from triplet-triplet annihilation (TTA). k_{tt} is the rate of TTA, which we set to approximately 10^{-14} cm^3 s^{-1} as reported in Ref. [31]. Φ^d_{tt} is the probability of product from the TTA interaction degrading. This will be energy dependent but using 10^{-8}, we obtain a fragmentation-rate constant of 10^{-22} cm^3 s^{-1}, consistent with that previously reported by Giebink *et al.* [27]. Equation (5) describes the

rate of degradation products arising from triplet-polaron quenching (TPQ). k_{tp} is the rate of TPQ, which is approximately 10^{-14} cm^3 s^{-1} [32]. Φ^d_{tp} is the probability of product from TPQ degrading, which if set to 10^{-10}, yields a fragmentation-rate constant associated with TPQ of 10^{-24} cm^3 s^{-1} consistent with Ref. [27]. In this case, the lower fragmentation is justified by the lower energy of the triplet-polaron pair compared to the triplet-triplet pair. For the cold (i.e., the molecule forms in its lowest excited state) and the hot-exciton cases, k^d_{ce} and k^d_{he} represent the rate of the degradation of a molecule from the populated excited state. This usually occurs in the picosecond regime and therefore a rate of approximately 10^{11} s^{-1} is assigned to both. For excited molecules, the typical photodestruction quantum yield (PQY) is approximately 10^{-4}–10^{-6} measured in solution [33–35] and about 10^{-9} in OLED devices [27,36] but as this will be the lowest excess energy of all three scenarios, Φ^d_{ce} and Φ^d_{he} are expected to be the smaller than Φ^d_{tt} and Φ^d_{tp}.

Within these constraints, assuming a polaron and triplet density of 10^{18} cm^{-3}, we find $[\dot{F}]_{tt} = 10^{14}$ cm^{-3} s^{-1} and $[\dot{F}]_{tp} = 10^{12}$ cm^{-3} s^{-1}. Consequently, assuming the hot-exciton yield of 1% discussed above, $[\dot{F}]_{he}$ will remain larger even if Φ^d_{he} becomes as small as 10^{-12}. If the hot-exciton yield is 1%, the cold-exciton population will be 2 orders of magnitude larger and therefore this pathway could be considered more significant if $\Phi^d_{ce}/100 > \Phi^d_{he}$. Wavelength-dependent PQY measurements are rare but previous work [35] has demonstrated changes of 2–3 orders of magnitude over a 0.5-eV energy range.

Given this analysis, Fig. 3 shows the relative contributions of each process to device degradation as a function of the PQY of the hot excitons (assuming that the PQY for cold excitons is 3 orders of magnitude smaller). In all cases, the hot-exciton degradation process is competitive with TTA and TPQ. Consequently, we expect the hot-exciton pathway to be competitive with these other mechanisms, since only a very small fraction of the formed excitons need to cause bond dissociation and the proposed mechanism does not require diffusion, unlike the biexcitonic processes. Kondakov *et al.* [37] have identified the excited states of the common host material 4,4'-bis(9-carbazolyl)-2,2'-biphenyl (CBP) as unstable and as the origin of degradation in their devices, ruling out biexcitonic processes based upon the observation of a linear dependence of the CBP photoreaction rate on the intensity of irradiation in films and in solutions. This conclusion has been challenged by Giebink *et al.* [27], who have asserted that their density in devices was very low due to rapid energy transfer from the CBP host to the guest. However, in our proposed mechanism, the degradation could occur on the guest in either the singlet or triplet state and therefore there would be sufficient density to make it viable.
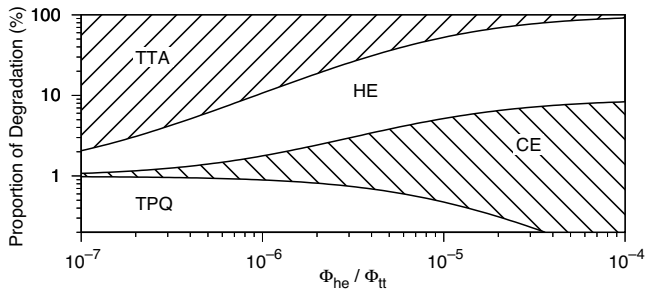
FIG. 3. A phase diagram showing the contribution of triplet-polaron quenching, cold excitons, hot excitons, and triplet-triplet annihilation to device degradation as a function of the PQY of the hot excitons. Here, the PQY of the cold excitons is assumed to be 3 orders of magnitude lower than that of the hot excitons.

Given the importance of the proposed mechanism, we now seek to gain further insight into the nature of the hot excitons formed. Figure 4 shows the distribution of excited states obtained during the simulations as a function of the relaxation rate between orbitals.

As shown in Fig. 1, the exciton (e_1, e_2, or e_3) formed depends on the relaxation rate between the orbitals. Nonradiative relaxation between close-lying energy states usually occurs on the femtosecond time scale [38], which is approximately 100 times faster than the hopping-attempt frequency used in the present work. However, in Fig. 4 we modify the ratio between the hopping-attempt frequency and the relaxation rate to assess its influence. With a high relaxation rate, i.e., in the infinite-relaxation limit, we expect that whenever a charged particle is in the HOMO $-$ 1 (LUMO $+$ 1) level, it will relax to the HOMO (LUMO) level 3 orders of magnitude faster than the hopping rates between molecules. In the other limit, where we assume that the relaxation rate tends to zero, i.e., in the zero-relaxation limit (ZRL), we expect a charged particle in the HOMO $-$ 1 (LUMO $+$ 1) level to have access to two pathways (see Fig. 5): it can hop onto an adjacent site or a second charged particle can hop onto the same site. Therefore, we expect the proportion of e_2 excitons to increase in the ZRL. We also expect to form e_3 states, i.e., where both charges populate excited orbitals and therefore form the highest energy exciton.

Figure 4 shows the number of e_1, e_2, and e_3 states formed as a function of the relaxation rate between orbitals. The population of e_2 increases toward the ZRL and to model the two limiting cases, we fit a sigmoid function,

$$f\left(k_{\mathbf{ii}}^{m0}\right) = C_0 + \frac{C_\infty - C_0}{1 + \left(k_X / k_{\mathbf{ii}}^{m0}\right)}, \tag{8}$$

where C_0 is the exciton count in the zero-relaxation limit, C_∞ is the exciton count in the infinite-relaxation limit,
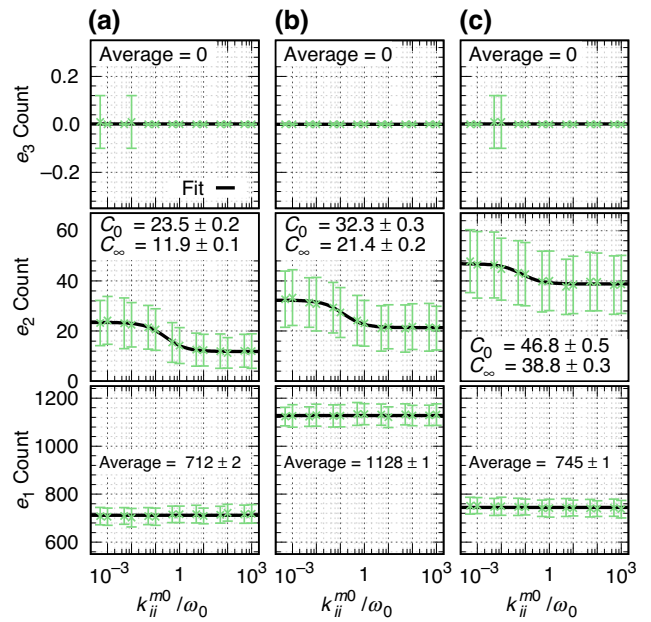
FIG. 4. A simulation of electrical selection: the total number of e_1 (lower panels), e_2 (middle panels), and e_3 (upper panels) excited states formed as a function of the relaxation rate between orbitals for a range of Gaussian DOS widths: (a) $\sigma/\Delta = 0.1$; (b) $\sigma/\Delta = 0.3$; (c) $\sigma/\Delta = 0.5$. The e_1 and e_3 populations show no dependence on the relaxation rate and so the average count is printed in each case. The e_2 populations are fitted with a sigmoid function. In each case, the zero-relaxation and infinite-relaxation limits of the function are printed and the crossing points are 0.25 ± 0.03, 0.13 ± 0.02, and 0.07 ± 0.02 from left to right.

and k_X is the crossing point (where the count is halfway between the two limits). All three are treated as fitting parameters and are reported in Fig. 4.

This clearly demonstrates that the probability of e_2 increases in the ZRL—i.e., when the charge resides in the excited state for longer it is more likely to form a hot exciton—and the switching point of the sigmoid function occurs when the relaxation rate between the orbitals is equal to the hopping rates between molecules. In contrast, the probability of e_3 is independent of the relaxation rate and is always zero. This because if the probability for a charge particle to populate an excited energy level is P, then the probability of excitons in the e_2 state is proportional to P. In contrast, as the e_3 states require both particles to populate an excited energy level, the probability becomes proportional to P^2. For most of the systems studied, we have found that the population of e_2 states is approximately 2%, which would suggest that an e_3 would occur at most once every 2500 excitons (0.04%). This highlights that not all higher-lying excitons are equally likely to form, which we term *electrical selection*, and therefore the character of the excited states must be considered within the hot-exciton picture.
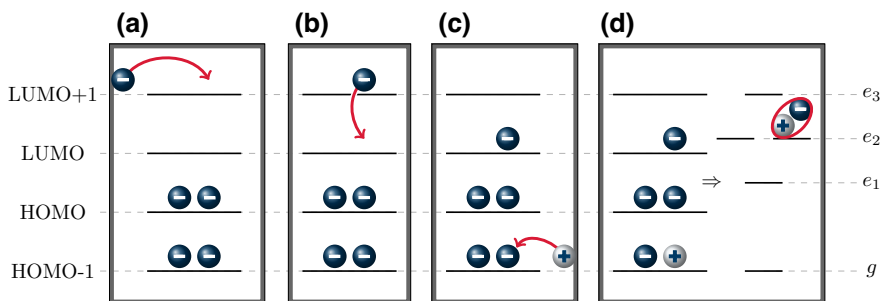
FIG. 5. A schematic of a proposed mechanism for hot-exciton formation. In this case, it is applied to electron trapping occurring first but it is equally valid for hole trapping. (a) The electron is transferred into the LUMO + 1 orbital. (b) Relaxation occurs so that the electron relaxes into the LUMO orbital. (c) The hole is transferred and trapped in the HOMO − 1 orbital, which (d) forms a hot-exciton state, e_2.

IV. DISCUSSION AND CONCLUSIONS

In this paper, we have used KMC simulations to investigate the mechanism of hot-exciton formation during electrical excitation relevant to the operation of OLEDs. This mechanism, illustrated schematically in Fig. 5, exploits the fact that the motion of charges through an organic semiconductor is not restricted to the HOMO and LUMO orbitals but, depending on the intrinsic energetic disorder, can populate higher-energy orbitals, such as HOMO − 1 and LUMO + 1. Our simulations have demonstrated that even for comparatively large energy gaps (>0.5 eV) there is a non-negligible probability of forming these hot-exciton states during charge recombination. As expected, this probability increases as the energy gap between the states decreases, although we anticipate that the higher probability low-energy excited states will be less significant than their less probable higher-energy counterparts because: (i) the excess energy associated with these higher-lying states will increase the propensity for degradation, especially for blue OLEDs, which operate close to molecular-dissociation thresholds, and (ii) for hot excitons only slightly higher in energy than the lowest excited states, one would expect very short lifetime, as they will more likely undergo internal conversion to the lowest exciton state.

The mechanism proposed and the associated KMC simulations also reveal insight into the types of excitons formed, as not all states are not equally likely to be formed, a process that we term *electrical selection*. Indeed, even for small energy gaps, the formation of the e_3 state is vanishingly rare. This state is of character (HOMO − 1 → LUMO + 1) and so to form, the second charge-trapping event has to occur faster than the excited state can relax [see Fig. 5(b)]. Throughout our simulations, even for long relaxation times, this state is not observed.

In summary, our KMC simulations have revealed a mechanism for hot-exciton formation upon charge recombination, which could increase the efficiency of OLEDs in a similar way to other recently proposed mechanisms [16]. However, the higher-energy states will also increase the susceptibility, especially of blue OLEDs, for the materials to undergo degradation. Throughout this work, we have neglected differentiating between states of different spin multiplicity, as the proposed mechanism can act independently of the spin state. However, we expect that it will play a more significant role for triplet states, as the population of higher-lying states scales with the energy gap between the states and molecules usually exhibits a higher density of low-lying triplet states.

Ultimately, this work hopefully opens new directions of research that must be considered when seeking to develop high-performance stable electroluminescent materials, especially for the pure-blue and deep-blue OLEDs. We anticipate that the hot-exciton mechanism will compete alongside other established mechanisms, such as biexcitonic and exciton-polaron quenching, that are commonly invoked to describe degradation in OLEDs. However, in contrast to these aforementioned mechanisms, the hot-exciton mechanism is unavoidable, as it happens upon the formation of excitons, which is a required step in OLEDs, i.e., light emission cannot happen without it. Ultimately, our proposal will hopefully motivate detailed experimental investigations and for this, wavelength-dependent PQYs [34], preferably in the solid state, should provide valuable insight.

[1] Y. Hou, X. Zhang, K. Chen, D. Liu, Z. Wang, Q. Liu, J. Zhao, and A. Barbon, Charge separation, charge recombination, long-lived charge transfer state formation and intersystem crossing in organic electron donor/acceptor dyads, J. Mater. Chem. C **7,** 12048 (2019).

[2] M. Gilbert and B. Albinsson, Photoinduced charge and energy transfer in molecular wires, Chem. Soc. Rev. **44,** 845 (2015).

[3] J. B. Burkholder, R. Cox, and A. Ravishankara, Atmospheric degradation of ozone depleting substances, their substitutes, and related species, Chem. Rev. **115,** 3704 (2015).

[4] A. Harris, J. Brown, and C. Harris, The nature of simple photodissociation reactions in liquids on ultrafast time scales, Annu. Rev. Phys. Chem. **39,** 341 (1988).

[5] G. A. Jones, A. Acocella, and F. Zerbetto, On-the-fly, electric-field-driven, coupled electron- nuclear dynamics, J. Phys. Chem. A **112,** 9650 (2008).

[6] S. Magnier, M. Persico, and N. Rahman, Quantum wavepacket dynamics simulations of above-threshold dissociation in Na_2^+, Chem. Phys. Lett. **279,** 361 (1997).

[7] A. Giusti-Suzor, F. H. Mies, L. F. DiMauro, E. Charron, and B. Yang, Dynamics of H_2^+ in intense laser fields, J. Phys. B: At., Mol. Opt. Phys. **28,** 309 (1995).

[8] T. Godfrey, H. Yu, M. S. Biddle, and S. Ullrich, A wavelength dependent investigation of the indole photophysics via ionization and fragmentation pump-probe spectroscopies, Phys. Chem. Chem. Phys. **17,** 25197 (2015).

[9] L. Rothberg, M. Yan, F. Papadimitrakopoulos, M. Galvin, E. Kwock, and T. Miller, Photophysics of phenylenevinylene polymers, Synth. Met. **80,** 41 (1996).

[10] J. Suchan, D. Hollas, B. F. Curchod, and P. Slavíček, On the importance of initial conditions for excited-state dynamics, Faraday Discuss. **212,** 307 (2018).

[11] H. Yersin, *Highly Efficient OLEDs: Materials Based on Thermally Activated Delayed Fluorescence* (John Wiley & Sons, Weinheim, Germany, 2019).

[12] M. A. Baldo, D. O'brien, M. Thompson, and S. Forrest, Excitonic singlet-triplet ratio in a semiconducting organic thin film, Phys. Rev. B **60,** 14422 (1999).

[13] C. Rothe, S. King, and A. Monkman, Direct measurement of the singlet generation yield in polymer light-emitting diodes, Phys. Rev. Lett. **97,** 076602 (2006).

[14] J. S. Wilson, A. Dhoot, A. Seeley, M. S. Khan, A. Köhler, and R. H. Friend, Spin-dependent exciton formation in π-conjugated compounds, Nature **413,** 828 (2001).

[15] M. Wohlgenannt, K. Tandon, S. Mazumdar, S. Ramasesha, and Z. Vardeny, Formation cross-sections of singlet and triplet excitons in π-conjugated polymers, Nature **409,** 494 (2001).

[16] W. Li, Y. Pan, L. Yao, H. Liu, S. Zhang, C. Wang, F. Shen, P. Lu, B. Yang, and Y. Ma, A hybridized local and charge-transfer excited state for highly efficient fluorescent oleds: Molecular design, spectral character, and full exciton utilization, Adv. Opt. Mater. **2,** 892 (2014).

[17] M. Segal, M. Singh, K. Rivoire, S. Difley, T. Van Voorhis, and M. Baldo, Extrafluorescent electroluminescence in organic light-emitting devices, Nat. Mater. **6,** 374 (2007).

[18] S. Difley, D. Beljonne, and T. Van Voorhis, On the singlet-triplet splitting of geminate electron-hole pairs in organic semiconductors, J. Am. Chem. Soc. **130,** 3420 (2008).

[19] Y. Xu, X. Liang, X. Zhou, P. Yuan, J. Zhou, C. Wang, B. Li, D. Hu, X. Qiao, and X. Jiang, *et al.*, Highly efficient blue fluorescent oleds based on upper level triplet-singlet intersystem crossing, Adv. Mater. **31,** 1807388 (2019).

[20] T. Northey, T. Keane, J. Eng, and T. Penfold, Understanding the potential for efficient triplet harvesting with hot excitons, Faraday Discuss. **216,** 395 (2019).

[21] J. S. Ward, N. A. Kukhta, P. L. Dos Santos, D. G. Congrave, A. S. Batsanov, A. P. Monkman, and M. R. Bryce, Delayed blue fluorescence via upper-triplet state crossing from C—C bonded donor-acceptor charge transfer molecules with azatriangulene cores, Chem. Mater. **31,** 6684 (2019).

[22] Y. Xu, P. Xu, D. Hu, and Y. Ma, Recent progress in hot exciton materials for organic light-emitting diodes, Chem. Soc. Rev. **50,** 1030 (2021).

[23] J. Liu, Z. Li, T. Hu, X. Wei, R. Wang, X. Hu, Y. Liu, Y. Yi, Y. Yamada-Takamura, and Y. Wang, *et al.*, Experimental evidence for "hot exciton" thermally activated delayed fluorescence emitters, Adv. Opt. Mater. **7,** 1801190 (2019).

[24] S. Scholz, D. Kondakov, B. Lussem, and K. Leo, Degradation mechanisms and reactions in organic light-emitting devices, Chem. Rev. **115,** 8449 (2015).

[25] K. Guo, C. Lin, Y. Wu, S. Xiao, X. Qiao, D. Yang, Y. Dai, Q. Sun, J. Chen, and D. Hu, *et al.*, Understanding of degradation mechanism by exciton dynamics and enhancement of operational lifetime by exciton management in blue fluorescent oleds based on hybridized local and charge-transfer molecule, Adv. Opt. Mater. **11,** 2202988 (2023).

[26] J. Lee, C. Jeong, T. Batagoda, C. Coburn, M. E. Thompson, and S. R. Forrest, Hot excited state management for long-lived blue phosphorescent organic light-emitting diodes, Nat. Commun. **8,** 15566 (2017).

[27] N. C. Giebink, B. D'andrade, M. Weaver, P. Mackenzie, J. Brown, M. Thompson, and S. Forrest, Intrinsic luminance loss in phosphorescent small-molecule organic light emitting devices due to bimolecular annihilation reactions, J. Appl. Phys. **103,** 044509 (2008).

[28] N. C. Giebink, B. D'Andrade, M. Weaver, J. Brown, and S. Forrest, Direct evidence for degradation of polaron excited states in organic light emitting diodes, J. Appl. Phys. **105,** 124514 (2009).

[29] Q. Wang and H. Aziz, Degradation of organic/organic interfaces in organic light-emitting devices due to polaron-exciton interactions, ACS Appl. Mater. Interfaces **5,** 8733 (2013).

[30] T. Pope, Y. Giret, M. Fsadni, P. Docampo, C. Groves, and T. J. Penfold, Modelling the effect of dipole ordering on charge-carrier mobility in organic semiconductors, Org. Electron. **115,** 106760 (2023).

[31] M. A. Baldo, C. Adachi, and S. R. Forrest, Transient analysis of organic electrophosphorescence. II. Transient analysis of triplet-triplet annihilation, Phys. Rev. B **62,** 10967 (2000).

[32] R. Coehoorn, P. Bobbert, and H. Van Eersel, Förster-type triplet-polaron quenching in disordered organic semiconductors, Phys. Rev. B **96,** 184203 (2017).

[33] R. Hojo, D. M. Mayder, and Z. M. Hudson, Donor-acceptor materials exhibiting deep blue emission and thermally activated delayed fluorescence with tris(triazolo)triazine, J. Mater. Chem. C **9**, 14342 (2021).

[34] D. M. Mayder, C. M. Tonge, G. D. Nguyen, R. Hojo, N. R. Paisley, J. Yu, G. Tom, S. A. Burke, and Z. M. Hudson, Design of high-performance thermally activated delayed fluorescence emitters containing *s*-triazine and *s*-heptazine with molecular orbital visualization by STM, Chem. Mater. **34**, 2624 (2022).

[35] K. Lao and A. N. Glazer, Ultraviolet-b photodestruction of a light-harvesting complex, Proc. Natl. Acad. Sci. **93**, 5258 (1996).

[36] C. Hauenstein, S. Gottardi, E. Torun, R. Coehoorn, and H. van Eersel, Identification of OLED degradation scenarios by kinetic Monte Carlo simulations of lifetime experiments, Front. Chem. **9**, 1227 (2022).

[37] D. Kondakov, W. Lenhart, and W. Nichols, Operational degradation of organic light-emitting diodes: Mechanism and identification of chemical products, J. Appl. Phys. **101**, 024512 (2007).

[38] K. Khalili, L. Inhester, C. Arnold, R. Welsch, J. W. Andreasen, and R. Santra, Hole dynamics in a photovoltaic donor-acceptor couple revealed by simulated time-resolved x-ray absorption spectroscopy, Struct. Dyn. **6**, 044102 (2019).